# Measurements of spin-orbit perturbation in atomic rubidium through photoelectron angular distributions

Yi-Yian Yin and D. S. Elliott
*School of Electrical Engineering, Purdue University, West Lafayette, Indiana 47907*
(Received 5 August 1991)

We discuss measurements of the angular distributions of photoelectrons produced by photoionizing ground-state rubidium with light of wavelengths between 266 and 285.3 nm. The spin-oribit perturbation in this heavy element affects the ratio of the oscillator strength for excitation to the $P_{3/2}$ state to that for excitation to the $P_{1/2}$ state. For our measurements the electron energy approaches that of the Cooper minimum in the photoionization spectrum, the effect of which is to reduce the asymmetry parameter from the nonrelativistic value of 2. At the shortest wavelength for which we have measured these distributions, the cross section for ionization to the $\epsilon P_{1/2}$ state has nearly vanished.

PACS number(s): 32.80.Fb

In this article we discuss experimental measurements of photoelectron angular distributions resulting from the single-photon ionization of atomic rubidium from its ground state to energies in the vicinity of a Cooper minimum. These measurements clearly show the effect of spin-orbit coupling in the $p$ continuum. Photoelectron angular distributions are a sensitive probe of atomic wave functions and have been successfully used to study a wide variety of atomic interactions, including hyperfine-coupling-induced quantum beats [1,2], the ac Stark shift [3,4], configuration mixing in an alkaline-earth element (barium) [5], and phase shifts between continuum states [6,7]. The present work presents a set of measurements of the single-photon photoelectron angular distribution at a variety of energies from a single initial state of an alkali metal. This data shows a strong variation with energy of the asymmetry parameter $\beta$ from its nonrelativistic value of 2. Spin-orbit coupling causes the Cooper minima for excitation to the $\epsilon P_{1/2}$ and the $\epsilon P_{3/2}$ states to be displaced from one another, resulting in a rapid variation of the angular distribution with photon energy in this region.

The effect of the spin-orbit perturbation on the heavy alkali metals has long been recognized. The anomolous ratio of peak heights for the $6\,^2S_{1/2}\rightarrow n\,^2P_J$, for $J=\frac{3}{2}$ and $\frac{1}{2}$, transitions in cesium was first attributed to this perturbation by Fermi [8] in 1930. In the continuum, this perturbation is responsible for several phenomena. For example, Seaton [9] showed in 1951 that the shift of the Cooper minima for the $\epsilon P_{1/2}$ and $\epsilon P_{3/2}$ states results in a nonzero minimum in the photoionization cross section. Other effects include (1) the Fano effect [10] (the spin polarization of the photoelectrons when ionized with circularly polarized light), (2) the variation of the photoionization cross section of polarized atoms for left and right circularly polarized light [11], (3) the production of polarized photoelectrons when photoionizing polarized atoms with unpolarized light [11], and (4) the deviation of the photoelectron angular distribution from a pure $\cos^2\theta$ distribution [12–16], where $\theta$ is the angle between the linear polarization of the optical field and the propagation direction of the ejected electron. The angular distribution is typically described by the asymmetry parameter, $\beta$, where

$$\frac{d\sigma}{d\Omega}=\frac{\sigma}{4\pi}[1+\beta P_2(\cos\theta)]\ ,$$

and $P_2(x)=\frac{1}{2}(3x^2-1)$ is the second-order Legendre polynomial. For ionization of an $s$ electron, $\beta$ has been shown [12] to take the form

$$\beta=2\frac{R_{3/2}^2+2R_{1/2}R_{3/2}\cos(\delta_{3/2}-\delta_{1/2})}{2R_{3/2}^2+R_{1/2}^2}\ ,$$

where $R_J$ is the radial matrix element for the $n_0\,^2S_{1/2}\rightarrow\epsilon P_J$ transition, and $\delta_J$ is the phase shift of the continuum wave function. In the absence of spin-orbit coupling, $R_{3/2}=R_{1/2}$ and $\delta_{3/2}=\delta_{1/2}$, and the asymmetry parameter reduces to 2. The isotropic component of the angular distribution is zero in this case. It has been shown [15] that spin-orbit coupling has little effect on $\delta$, so we can safely set $\cos(\delta_{3/2}-\delta_{1/2})\cong 1$. $R_{3/2}$ and $R_{1/2}$ are affected by the spin-orbit perturbation, however, and as the photon energy is varied near the Cooper minimum, $R_{1/2}$ and $R_{3/2}$ each pass through zero, but at somewhat different energies. This leads to a rapid variation of $\beta$ with photon energy in this region.

Very few measurements of $\beta\neq 2$ for photoionization from $s$ states have been reported in the past. In 1931, Chaffee [17] reported an angular distribution measurement for potassium using light of wavelength 240 nm. He concluded that the distribution was very close to the expected $\cos^2\theta$ distribution, but examination of his data does indicate the presence of an isotropic component. Ong and Manson [15] reanalyzed Chaffee's data to obtain $\beta=1.5\pm 0.3$. Measurements of $\beta$ for photoionization of the $6s$ electron of mercury [18] have also been reported, showing possible effects of autoionizing resonances as well as spin-orbit coupling [19]. There has also been some activity, experimental [20,21] as well as theoretical

 

[22–25], concerning the angular distribution of the inner-shell photoionization of Xe, the $5s \rightarrow \epsilon p$ transition with photon energies in the range 26–40 eV. Recent calculations by Tulkki [25] indicate that multiple-electron excitation channels must be included to produce good agreement with experiment for photoionization cross sections and asymmetry parameters.

Finally, Cuéllar *et al.* [26] reported last year measurements of photoelectron angular distributions for two-photon resonant, three-photon ionization of atomic cesium. The intermediate state, $ns\ ^2S_{1/2}$, $n$ ranging from 8 to 12, was selected by tuning the wavelength of the dye-laser output. Since the $ns\ ^2S_{1/2}$ state was isotropically populated by the linearly polarized laser, the problem is essentially reduced to a single-photon ionization of the excited $S$ state, with one data point per $S$ state. Since the photoelectron energy is near the Cooper minimum in each of these cases, $\beta$ shows a strong deviation from the nonrelativistic value of 2.

In the present work, we have studied photoionization of an alkali metal, rubidium, to take advantage of the relative simplicity afforded by a single ground-state $s$ electron in the outer shell. We have used light in the ultraviolet so that the rubidium is ionized through the absorption of a single photon. By varying the wavelength of the laser, we have studied the energy dependence of $\beta$, with all data corresponding to the ionization of a single state, the ground state.

The dye-laser system in this experiment consists of a tunable oscillator and three amplifiers which are pumped by the second harmonic of a Nd:YAG laser. The dye oscillator, in a Littman [27] configuration, is pumped longitudinally. The laser cavity is very short ($\approx 5$ cm), so the laser typically operates on only one or two longitudinal modes. This laser provides up to 50 mJ in a $TEM_{00}$ mode and displays relatively good stability.

The optical system and photoelectron detection system are shown in Fig. 1. A high-quality polarizer is inserted after the last stage of the amplifier to ensure the linearity of the laser polarization to better than 1000:1. In order to get a tunable ultraviolet laser beam in the range from 275.3 to 285.3 nm, the dye-laser beam is focused by a 100-cm focal length lens into a $\beta$-$BaB_2O_4$ frequency-doubling crystal. This crystal has a 48° cut angle and high-damage threshold of 5 GW/cm$^2$. Proper laser focusing is important to get sufficient second-harmonic output, and at the same time prevent damage of the crystal. The data point at 266 nm was determined using the fourth harmonic of the Nd:YAG laser. A half-wave Fresnel rhomb was used to rotate the polarization direction of laser beam because of its wide wavelength range. The degree of linear polarization of the rotated beam was measured to be better than $10^3$:1.

The vacuum system consists of two chambers, the oven chamber and the interaction chamber. The former contains an oven and nozzle which serve as the atom source. A pair of 1-mm-diam apertures separated by 28 cm produced a collimated beam. The oven and nozzle were heated to a temperature of ~160° and 190 °C, respectively. The nozzle is intended to decrease the density of rubidium dimers in the beam [28]. The oven chamber is pumped by a 4-in. diffusion pump and cryotrap to a typical pressure of $2\times10^{-7}$ Torr. The pressure is more critical in the interaction chamber since ionization of background gas by the uv radiation can easily mask the rubidium signal. In this chamber we use a 6-in. cryopump, assisted by a small turbo molecular pump in parallel, to attain a vacuum of $4\times10^{-8}$ Torr. At this pressure, background counts detected by the electron detector are reduced to less than one per 600 laser pulses. The interaction region is defined by the intersection of the atomic beam and the uv beam. Each has a diameter of approximately 1 mm. The atomic beam density is calculated to be $\sim 1.2\times10^7$ cm$^{-3}$. The crossing angle between the two beams is 108°. Electric and magnetic fields in the interaction region are reduced using a pair of electrically grounded nonmagnetic stainless-steel parallel plates spaced by 2.75 cm, and three pairs of 90-cm-diam Helmholtz coils, respectively. The lower grounded plate was constructed of a fine mesh (82% transmitting, 50 threads per inch) to facilitate pumping. The upper plate had a 2.2-mm-diam aperture, above which an electron lens and channel electron multiplier were mounted. The size of this aperture and that of the interaction region define the angular resolution of our measurements, which we estimate to be approximately 0.18 rad (10°).

The photoelectron angular distributions were determined by measuring the electron current transmitted by

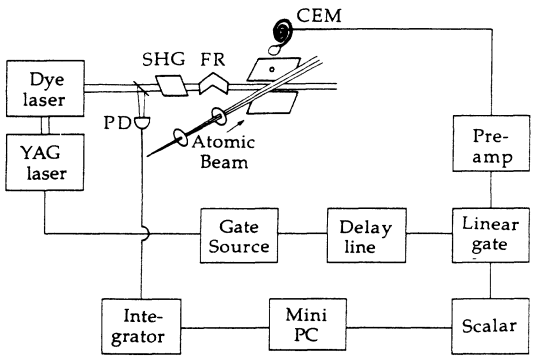


FIG. 1. Experimental configuration. PD, photodiode; SHG, second harmonic generating crystal; FR, half-wave Fresnel rhomb; CEM, channel electron multiplier.

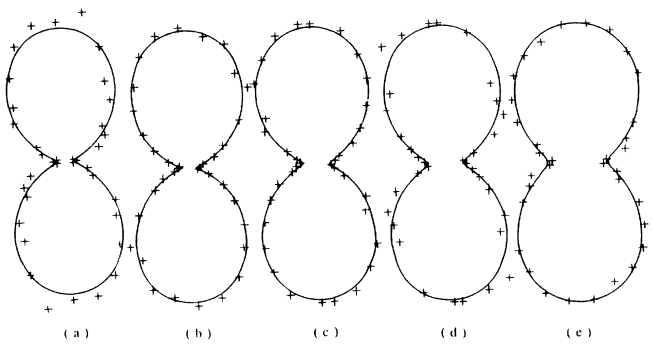


FIG. 2. Photoelectron angular distributions. The laser polarization is in the vertical direction. The wavelength of the laser for these distributions was (a) 285.3, (b) 284.0, (c) 280.3, (d) 275.3, and (e) 266.0 nm.

TABLE I. $\beta$ values for the different laser wavelengths.

| $\lambda$ (nm) | $\beta$ | $\Delta\beta$ |
|---|---|---|
| 285.3 | 1.739 | 0.036 |
| 283.5 | 1.704 | 0.021 |
| 280.3 | 1.602 | 0.031 |
| 275.3 | 1.395 | 0.036 |
| 266.0 | 1.132 | 0.023 |

the aperture as a function of the direction of polarization of the uv beam. The power of the uv beam and the density of the atomic beam were adjusted to a level such that the maximum probability of detecting an electron per laser shot was $\sim 0.17$. The gated pulse detection electronics were configured so as to determine the fraction of pulses for which at least one electron was detected. A correction for pileup errors (caused by the arrival of two or more electrons), assuming Poisson statistics, was applied. The maximum correction was about 8%. Electron counts were accumulated for 1000–1800 laser pulses at each polarization direction, with polarizations spaced by about 10°. Since the laser polarization rotates by twice the rotation angle of the Fresnel rhomb, effects due to displacement of the laser beam could be checked by accumulating data over the full 360° rotation range of the rhomb. No disparity was observable between the data in the first half of the rotation and the data in the second half. The polar plots in which the data is displayed, Fig. 2, show the average of data for the polarization at the angle $\theta$ and the angle $\theta+180°$. The standard deviation of each data point, calculated by the scatter in the count rate taken over several subsets of data at each angle is consistent with the shot noise limit $\sigma \sim \sqrt{n}$, where $n$ is the number of detected electrons. The solid line in each figure is the result of a least-squares fit to the data. We have chosen to fit the data to a curve of the form

$$\frac{d\sigma}{d\Omega} = a_0 + a_1 \cos 2\theta$$

because of the orthogonality of the harmonics over the interval $0-2\pi$. We applied a correction for the finite aperture size ($\leq 1\%$), and derived our final results for $\beta$ and $\Delta\beta$ from the corrected fitting parameters $a_0$ and $a_1$ and their uncertainties. These results are presented in Table I and in Fig. 3. $\Delta\beta$ reported here is purely statistical, and represents a one $\sigma$ deviation. Figure three also shows three other data sets. The dot-dashed line is the result of a Dirac-Fock calculation by Ong and Manson [15]. This curve shows a rapid variation of $\beta$ from a value close to two for low-electron energies to $-1$, and then an increase gain to 2 for large electron energy. The energy at which the dip occurs appears to be off, a possibility the authors anticipated because of the omission of correlation effects and the complete Breit effect. The other two curves are derived from the results of studies of

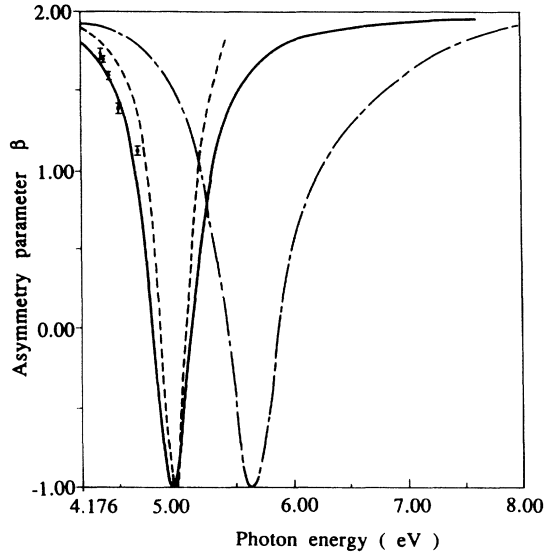


FIG. 3. Asymmetry parameter, $\beta$, vs photon energy. The data points represent the results of the present work. The dot-dashed line is the Hartree-Fock result from Ong and Manson [15]. The two other data curves are derived from the results of studies of polarization effects, as reported in Refs. [11] (dashed) and [29] (solid).

polarization effects. These results were reported in terms of the Fano parameter, $x=(2R_{3/2}+R_{1/2})/(R_{3/2}-R_{1/2})$, which we have converted to $\beta$. The dashed line represents the experimental results of Baum, Lubell, and Raith [11], who measured the ionization intensity asymmetries for polarized atoms using right or left circularly polarized light. The quoted uncertainty on these measurements is approximately 5–10 times larger than ours, and agreement of these results with ours is consistent within this accuracy. The solid line in Fig. 3 is the result of a semiempirical calculation by Weisheit [29]. Our data are in excellent agreement with these results.

The present work clearly shows the effect of $LS$ coupling on the photoelectron distribution for an alkali metal in the vicinity of the Cooper minimum. At the shortest wavelength for which we have measured these distributions, the cross section for ionization to the $\epsilon P_{1/2}$ state has nearly vanished, making $\beta$ very close to 1. We plan to extend our measurements to shorter wavelengths in order to cover the entire range of the Cooper minimum. Extension of the wavelength range would be useful to follow $\beta$ to $-1$ (corresponding to a $\sin^2\theta$ angular distribution), with a subsequent increase.

Useful discussions and assistance by Ce Chen, L. A. Westling, and A. V. Smith have been helpful in this work. This work was supported by the National Science Foundation Grant No. ECS-8451259.

[1] M. Strand, J. Hansen, R.-L. Chien, and R. S. Berry, Chem. Phys. Lett. **59**, 205 (1978).
[2] G. Leuchs, S. J. Smith, E. Khawaja, and H. Walther, Opt. Commun. **31**, 313 (1979).
[3] S. N. Dixit and P. Lambropoulos, Phys. Rev. Lett. **46**, 1278 (1981); Phys. Rev. A **27**, 861 (1983).
[4] W. Ohnesorge, F. Diedrich, G. Leuchs, D. S. Elliott, and H. Walther, Phys. Rev. A **29**, 1181 (1984).
[5] E. Matthias, P. Zoller, D. S. Elliott, N. D. Piltch, S. J. Smith, and G. Leuchs, Phys. Rev. Lett. **50**, 1914 (1983).
[6] P. Lambropoulos and M. R. Teague, J. Phys. B **9**, 587 (1976).
[7] H. Kaminski, J. Kessler, and K. J. Kollath, Phys. Rev. Lett. **45**, 1161 (1980).
[8] E. Fermi, Z. Phys. **59**, 680 (1930).
[9] M. J. Seaton, Proc. R. Soc. London, Ser. A **208**, 418 (1951).
[10] U. Fano, Phys. Rev. **178**, 131 (1969); **184**, 250 (1969).
[11] G. Baum, M. S. Lubell, and W. Raith, Phys. Rev. Lett. **25**, 267 (1970).
[12] T. E. H. Walker and J. T. Waber, Phys. Rev. Lett. **30**, 307 (1973); J. Phys. B **6**, 1165 (1973); **7**, 674 (1974).
[13] G. V. Marr, J. Phys. B **7**, L47 (1974).
[14] K.-N. Huang and A. F. Starace, Phys. Rev. A **19**, 2335 (1979).
[15] W. Ong and S. T. Manson, Phys. Rev. A **20**, 2364 (1979).
[16] M. S. Pindzola, Phys. Rev. A **32**, 1883 (1985).
[17] M. A. Chaffee, Phys. Rev. **37**, 1233 (1931).
[18] A. Niehaus and M. W. Ruf, Z.Phys. **252**, 84 (1972).
[19] D. Dill, Phys. Rev. A **7**, 1976 (1973).
[20] J. L. Dehmer and D. Dill, Phys. Rev. Lett. **37**, 1049 (1976).
[21] M. G. White, S. H. Southworth, P. Kobrin, E. D. Poliakoff, R. A. Rosenberg, and D. A. Shirley, Phys. Rev. Lett **43**, 1661 (1979).
[22] W. Ong and S. T. Manson, J. Phys. B **11**, L65 (1978); Phys. Rev. A **19**, 688 (1979).
[23] W. R. Johnson and K. T. Cheng, Phys. Rev. Lett. **40**, 1167 (1978); Phys. Rev. A **20**, 978 (1979).
[24] K.-N. Huang and A. F. Starace, Phys. Rev. A **21**, 697 (1980).
[25] J. Tulkki, Phys. Rev. Lett. **62**, 2817 (1989).
[26] L. E. Cuéllar, R. N. Compton, H. S. Carmin, Jr., and C. S. Feigerle, Phys. Rev. Lett. **65**, 163 (1990).
[27] M. G. Littman, Appl. Opt. **23**, 4465 (1984).
[28] M. Lambropoulos and S. E. Moody, Rev. Sci. Instrum. **48**, 131 (1977).
[29] Jon L. Weisheit, Phys. Rev. A **5**, 1621 (1972).